# Application of sequential extractions and X-ray absorption spectroscopy to determine the speciation of chromium in Northern New Jersey marsh soils developed in Chromite Ore Processing Residue

Evert J. Elzinga* and Ashley Cirmo

Department of Department of Earth & Environmental Sciences

Rutgers, The State University of New Jersey

Newark, NJ 07102

USA

* Corresponding author. Telephone: 973 353 5238; Email: elzinga@andromeda.rutgers.edu

**ABSTRACT**

The Cr speciation in marsh soils developed in weathering chromite ore processing residue (COPR) was characterized using sequential extractions and synchrotron microbeam and bulk X-ray absorption spectroscopic (XAS) analyses. The sequential extractions suggested substantial Cr associated with reducible and oxidizable soil components, and significant non-extractable residual Cr. Notable differences in Cr speciation estimates from three extraction schemes underscore the operationally defined nature of Cr speciation provided by these methods. Micro X-ray fluorescence maps and μ-XAS data indicated the presence of μm-sized chromite particles scattered throughout the weathered COPR matrix. These particles derive from the original COPR material, and have relatively high resistance towards weathering, and therefore persist even after prolonged leaching. Bulk XAS data further indicated Cr(III) incorporated in $Fe(OH)_3$, and Cr(III) associated with organic matter. The low Cr contents of the weathered material (200-850 ppm) compared to unweathered COPR (20000 - 60000 ppm) point to substantial Cr leaching during COPR weathering, with partial repartitioning of released Cr into secondary $Fe(OH)_3$ phases and organics as Cr(III). The effects of anoxia on Cr speciation, and the potential of active COPR weathering releasing Cr(VI) deeper in the profile requires further study.

# 1. INTRODUCTION

Chromite ore processing residue (COPR) is the waste product of high-temperature lime roasting of chromite ore to isolate and extract Cr as soluble $Na_2CrO_4$ salt. The residue has been produced in large quantities worldwide at chromate salt production centers in urban industrial areas in Europe and the US such as Glasgow, U.K., and Jersey City, New Jersey, USA, as well as at chromite ore processing plants operating in Japan, India, Pakistan and the former Soviet Union [1-4]. Due to its sand-like physical properties, COPR was considered a suitable material for use as foundation material and wetland backfill, and was widely introduced into urban environments, commonly at sites that currently serve residential, commercial or industrial purposes and have high real estate value [1, 4-7]. The environmental impacts of these COPR deposits are not well understood. Residual Cr contents of COPR are in the in 2-6 wt% range, and of concern is the presence of hexavalent Cr(VI), a strong carcinogen and mutagen, which may account for up to 35% or more of total residual Cr in COPR [8-11]; the remainder is Cr(III), which is less problematic because it is a micronutrient with much lower toxicity and solubility than Cr(VI). Under aqueous conditions at the Earth's surface, COPR is not stable, and will undergo weathering reactions that release Cr(VI) [4, 6, 12-16]; consequently, COPR deposits are an important source of Cr contamination of nearby soils, sediments, surface and groundwaters [e.g. 3, 13, 17, 18].

The mineralogy of COPR is initially dominated by high-temperature oxides such as brownmillerite ($Ca_2FeAlO_5$) and periclase (MgO), which are formed during ore roasting [10]. The material is strongly alkaline, with an equilibrium pH of 11.5-12.5 for water in contact with COPR. Postdepositional transformations induced by hydration under surface conditions produce secondary minerals along a reaction trajectory that includes the formation of calcite, brucite, hydrocalumite, and hydrogarnet as well amorphous $SiO_2$ and cementing agents such as $Ca_3Al_2O_6$ in the early stages of weathering under alkaline conditions, and formation of amorphous Fe(III)- and Al-oxides at more

advanced stages of weathering associated with lower pH values [9, 10, 12, 13, 19]. Major Cr(VI) host phases in COPR are hydrogarnet and Mg/Ca-Al layered double hydroxide phases, whereas Cr(III) is present in residual (non-transformed) chromite ($FeCr_2O_4$) and Cr(III)-substituted brownmillerite [4, 10, 11, 20, 21]. Leaching of Cr(VI) results from destabilization and dissolution of Cr(VI)-bearing minerals during weathering [4, 12]. The acid neutralizing capacity of COPR is high with respect to leaching to typical surface and groundwater pH conditions [e.g. 4, 12, 16, 22, 23], and therefore long leaching times and/or extensive acid inputs are required to reach equilibrium.

The aim of the current study was to investigate the solid state Cr speciation at a former COPR dump site in Northern New Jersey. Between 1905 and 1971, three chromite ore processing plants were operational in Jersey City and Kearny for chemical manufacturing of chromate and bichromate. These plants generated over 2 million tons of COPR waste that was disposed throughout the Northern New Jersey Area [1, 5]. The New Jersey Department of Environmental Protection has identified over 160 sites contaminated with COPR in Hudson and Essex Counties, many of which are located in urban residential areas [5]. The site of the current study is located in the New Jersey Meadowlands, a wetland area near the New Jersey/New York harbor. The site received COPR deposits in the past, but was not completely filled in and remains a brackish marsh that is submerged for substantial portions of the year. The COPR deposits at this location have been weathering for over 40 years, and the aim of the current study was to assess the resulting Cr speciation in the deposit top layers, which have seen the most intense weathering. We refer to these top layers as soils, since, despite their unusual parent material, they show clear signs of pedogenetic alterations to the COPR parent material resulting from biological activity and chemical weathering, and they serve the same functions as natural wetland soils (sustaining plant growth, habitat of subsurface flora and fauna, support of man-made structures, etc.) in the area. The chemical speciation of Cr in the COPR soils was characterized with a combination of sequential extraction experiments and synchrotron-based spectroscopic analyses. We report evidence for

substantial repartitioning and leaching of Cr in these weathered COPR deposits. The results of the current study are likely to be applicable to numerous other sites where COPR was used as fill-in material of marshlands in New Jersey and elsewhere.

## 2. MATERIALS AND METHODS

### 2.1 Soil sample collection and characterization

Soil samples were collected from Kearny Brackish Marsh in the New Jersey Meadowlands. The site is to a large extent submerged and bordered to the east by the Hackensack river. A dike runs through the site in a roughly North-South direction, whereas the New Jersey Turnpike overpasses the site West-East. Sampling was done from the dike, using a spade to collect the top 15 cm of soil at 13 sites along a stretch of approximately 250 m. At the time of sampling (July, 2008), the area adjacent to the dike was not submerged, and the water table was approximately 10-15 cm below the soil surface at the sampling locations. The samples were transported to the Rutgers-Newark campus, where they were dried for 24 h, and then sieved to <1 mm. The sieved materials were measured for pH by suspending 5 g of material in 5 mL of water;  suspensions were shaken for 10 min and allowed to settle before pH was measured in the supernatants [24].

The organic content of the samples was determined using the loss on ignition (LOI) method described by Nelson and Sommers [25], which involves combustion at 400 °C following sample drying at 105 °C. Microwave-assisted extraction using concentrated $HNO_3$ was used to determine total contents of Cr and Fe in the samples. The method involved addition of 0.2 g of sample to 7 mL of concentrated $HNO_3$ (90%), followed by pressurized microwave heating for approximately 40 minutes. Following extraction, the supernatants were collected and analyzed for dissolved Cr and Fe using atomic absorption spectrometry (AAS); the Cr and Fe contents of the soil samples were calculated from the dissolved Cr and Fe concentrations, and the solid:solution ratio employed in the extraction.

**2.2 Sequential Extractions**

Three different sequential extraction schemes were employed for macroscopic assessment of the Cr speciation in the samples: (1) the scheme proposed by the Commission of the European Communities Bureau of Reference (BCR; reference [26]); (2) the scheme proposed by Tessier et al. [27]; and (3) the scheme proposed by Zeien and Brummer [28], and further described in references [29] and [30]. These schemes were selected because they have been widely used (both in original and modified forms) in previous studies concerned with metal speciation in soils and sediments [e.g. 29-32 and references therein]. Table 1 presents a summary of the three schemes as applied in the current study, and shows that they differ primarily in the number of different Cr species distinguished, and the types of solutes and extraction temperatures used to extract specific Cr species. The Zeien-Brummer scheme was modified from the original by omitting the first step targeting exchangeable and mobile metal soluble in $NH_4NO_3$ [28-30], based on the assumption that this fraction would be small for our soils and would be extracted in step 1 of the current scheme (which is the same as step 2 of the original scheme) aimed a readily mobilizable metal extractable in 1M $NH_4$- acetate of pH 6 (Table 1). The results from the schemes were compared with respect to the amounts of Cr extracted in similar steps (e.g. organically bound Cr as extracted in step 3 of the BCR and Zeien-Brummer schemes, and in step 4 of the Tessier scheme; Table 1); further constraints on the Cr speciation in the marsh soils were provided by the spectroscopic measurements discussed below.

Five samples from the total of 13 marsh samples collected were selected for the sequential extraction experiments; the selected soils had moderate to high Cr concentrations as determined from the acid digestions described above, and had varying Fe and organic matter levels and pH values. For the extractions, 1 gram of soil material was weighed into a 30 mL polypropylene centrifuge tube; each soil sample was run in triplicate. Extractions were performed using either a thermostatted water bath

with reciprocal shaker for high temperature extractions, or a regular reciprocal shaker for extractions performed at room temperature. Following each extraction step, the samples were centrifuged (20-30 minutes at 6000 rpm), and the supernatants were collected, filtered through 0.45 μm filters, and then acidified using concentrated $HNO_3$. The solids were washed between successive steps, and the washing solutions were combined with the original extractant solutions. The extractant solutions were analyzed by atomic absorption spectrometry (AAS) for dissolved Cr and Fe. For each extraction scheme, the residual Cr fractions were determined by microwave assisted digestion in concentrated $HNO_3$ of one of the triplicate samples run for each soil sample. The sum of extracted and residual Cr was generally within 15-20% of the total amount of Cr in the sample as determined from the initial digestions.

## 2.3 Synchrotron X-ray Analyses

Synchrotron based X-ray techniques were used in addition to the sequential extraction experiments described above to further characterize and constrain the Cr speciation in the marsh soil samples. We used spatially resolved X-ray fluorescence in combination with micro-focused and bulk X-ray absorption spectroscopy (XAS) measurements to determine the oxidation state and main coordination environment, as well as the dispersion pattern and elemental association(s) of Cr in the soil matrix.

Spatially resolved micro X-ray fluorescence (μ-SXRF) data were collected in combination with micro-focused X-ray absorption near-edge spectra on beamline X27A of the National Synchrotron Light Source (NSLS) at Brookhaven National Laboratory, Upton, New York. Single layer soil particles were captured on Kapton tape and mounted onto a slide frame. The frame was mounted on an XYZ motorized sample stage positioned at $45^0$ incidence to the beam. A Si(111) monochromator was tuned to provide monochromatic radiation (10.0 keV), and the beam was focused with Kirkpatrick-Baez micro-focusing mirrors to produce a $15 \times 15$ μm spot on the sample. The X-ray fluorescence signal was

detected by a single-element solid state Ge detector. Mapping was done over approximately 1.5 x 1.5 mm$^2$ areas with a step size of 15 μm and a dwell time of 5s per pixel by raster-scanning in 'step-and-repeat' mode [33]. Because of the difficulty in quantifying matrix effects for absolute abundance calculations in heterogeneous materials, we report elemental abundance in detector counts only, which documents qualitatively the relative abundance of elements.

Micro-focused near edge spectra were collected at selected spots in the XRF maps. The spectra were collected at the Cr K edge. Scanning was done using.steps and counting times of 2 eV and 4 s, 0.3 eV and 10 s, and 0.5 eV and 10 s in the 5970-5982 eV, 5983-6020 eV, and 6021-6060 eV energy ranges, respectively.

Bulk X-ray absorption spectroscopic measurements were performed at beamline X11A of the NSLS to determine the average oxidation state and coordination environment of Cr in the samples. Spectra were recorded at room temperature at the Cr K edge (5989 eV) using an Ar filled Stern-Heald detector and a 30 cm $I_0$ detector filled with a gas mixture of 80% He and 20% $N_2$. Scanning was done over the energy range -200 to +300 eV relative to the Cr K edge, with multiple spectra (5-10) recorded per sample to improve signal-to-noise. In addition to the marsh soil samples, a number of Cr reference materials were analyzed at Cr K edge as well to aid interpretation of the soil data. The references analyzed were the following: (1) aqueous Cr(VI) as a 0.05 M $Na_2CrO_4$ solution of pH 8.0; (2)aqueous Cr(III) as a 0.02 M $Cr(NO_3)_3.9H_2O$ solution of pH 3.0; (3) aqueous Cr(III)-humic acid, prepared as a solution of 0.005 M  solution of $Cr(NO_3)_3.9H_2O$ in combination with 1500 mg C L$^{-1}$ of Suwannee River Humic Acid at pH 4.5. In addition, the spectra of $Cr(OH)_3$ and of Cr(III) incorporated into $Fe(OH)_3$ with final formula $Cr_{0.1}Fe_{0.9}(OH)_3$ and $Cr_{0.3}Fe_{0.7}(OH)_3r(OH)_3$ were kindly provided by Dr. Yuanzhi Tang (Harvard University); preparation of these samples is described in [34]. The spectrum of spinel chromite ($FeCr_2O_4$) was kindly provided by Dr. Peter Nico (Lawrence Berkeley National Laboratory), and has previously been reported in [35] and [21].

Spectra of marsh soil samples and reference compounds were processed using the WinXAS 3.1 program [36]. Scans of individual samples were calibrated and averaged, and a linear function was fitted to the pre-edge and post-edge regions of the averaged spectrum for background removal and normalization. Linear combination fitting and principal component analysis of the background corrected normalized spectra were accomplished with the routines available for these analyses in WinXAS 3.1 using standard procedures [28, 37-39].


## 3. RESULTS

### 3.1 Soil Characteristics

The pH values, organic matter contents, and Fe and Cr levels of the 13 soil samples collected are summarized in Table 2. The soils have pH values that range from slightly acidic to near neutral (4.5-6.7), and Fe content ranging from 1.3 to 2.2 wt %; the organic matter contents range from 11-25 wt% (Table 2). The high organic matter contents reflect the wet conditions encountered in these marsh soils, which limit the rate and extent of organic matter decomposition; in fact, most of the samples contained non-humified organic debris (non-digested parts of roots and leafs) in addition to organic matter in more advanced stages of decomposition. The Cr contents in the soils ranged between 200 and 850 ppm (on a dry soil weight basis). While these values are substantially lower than the 15000-20000 ppm Cr contents reported for samples collected at this site in an earlier study [1], they exceed the 20 ppm soil clean-up criterion of the New Jersey Department of Environmental Protection for Cr(VI) at residential and non-residential sites, but are well below the NJDEP limit of 120,000 ppm limit for Cr(III) at residential sites [5, 21].

Correlations between the soil parameters presented in Table 1 were absent or weak. Figure 1 presents the (weak) correlation observed between Cr content and Fe content of the soils, with an $R^2$ value of 0.49, suggestive perhaps of partial control of Fe-containing minerals on Cr retention in these

soils. Correlations between Cr content and any other soil parameters had $R^2$ values < 0.1.

**3.2 Extraction Results**

The results obtained from the three sequential extraction schemes are presented in Figure 2. The mass balance between measured extracted and residual Cr in the extraction schemes and the measured total Cr in the samples generally agreed within 15-20%; to facilitate comparison of the extractions results between the soils and between the schemes, the Cr fractions are normalized to the total amount of Cr extracted.

Comparison of the data presented in Figure 2 indicates substantial differences in the extraction results from the three schemes. All three schemes extract quantitative amounts of Cr associated with Fe and Mn oxides (the reducible fractions in the BCR and Tessier schemes, and the combined Cr fractions 2, 4 and 5 in the Zeien-Brummer scheme), and leave substantial residual Cr, but notable differences exist between the schemes as to the absolute amounts and relative contributions of these Cr fractions in the marsh soils (Fig. 2). In addition, the BCR and Tessier schemes extract substantial Cr associated with oxidizable soil components (nominally organic matter), whereas the Zeien-Brummer scheme extracts only minor amounts of organically complexed Cr (Fig. 2). Of note is the consistently low amount of Cr extracted in acidic solutions in all three schemes (weakly bound Cr; fraction 1 of the BCR and Zeien-Brummer schemes, and fractions 1 and 2 of the Tessier scheme), which suggests a low fraction of readily accessible and highly soluble Cr in these soils.

Comparisons between the amounts of Cr extracted in comparable steps between the three schemes are presented in Figure 3 in the form of x-y correlation plots. The following Cr fractions are compared in this figure: (1) acid soluble Cr representing weakly bound and/or carbonate-associated Cr as extracted in step 1 of the BCR and Zeien-Brummer schemes, and in the combined steps 1 and 2 of the Tessier scheme (Fig. 3A); (2) Cr associated with Fe and Mn-oxides as extracted in step 2 of the

BCR scheme, step 3 of the Tessier scheme, and in the combined steps 2, 4, and 5 of the Zeien-Brummer scheme (Fig. 3B); (3) organically complexed Cr as extracted in step 3 of the BCR and Zeien-Brummer schemes, and in step 4 of the Tessier scheme (Fig. 3C); and (4) residual non-extracted Cr (Fig. 3D). The comparisons in Fig. 3 indicate generally positive correlations between the Cr fractions, but the correlations are not particularly strong, especially for the Cr fractions associated with reducible and organic soil fractions, and the plots clearly bring out the large differences in extracted Cr between the various schemes noted above. Although the relatively poor correlations may in part be due to the small number of samples characterized here, the large differences in the amounts of Cr extracted in comparable steps point to important differences in the selectivity and efficiency of extractants used in the various schemes, and underscore the well-known fact that sequential extraction schemes provide estimates of operationally defined Cr species [40-43]. Despite these differences, however, the combined results from the three extraction schemes suggest that Fe(III)-(hydr) oxides and possibly organic matter play an important role in Cr retention in these soils, and indicate that a substantial fraction of Cr in these soils is not readily available for extraction. Results from X-ray absorption spectroscopic analyses of Cr speciation presented next proved useful in evaluating the results from the sequential extraction schemes.

### 3.3 μ-XRF and μ-XAS results

Figure 4 presents the X-ray fluorescence (XRF) maps of the Cr, Fe and Ca dispersion patterns in three representative soils analyzed in this study. The Fe maps indicate widespread distribution and high intensity counts of Fe in these samples, consistent with the high Fe content of the soils (Table 2). The distribution of Ca is less widespread, and appears to be mostly independent of the Fe distribution patterns, although overlap between Fe and Ca hotspots occurs in some locations (Fig. 4). Chromium distributions are characterized by small intense hotspots scattered throughout the matrix that are for the

most part unrelated to Fe and Ca hotspots; at some locations, however, overlap between Cr and Fe hotspots occurs (Fig. 4).

Micro-focused X-ray absorption near edge spectra at the Cr K edge were recorded at the numbered Cr hotspots indicated in Fig. 4. The spectra are presented in Figure 5, and compared to the spectra of the $Fe_{0.1}Cr_{0.9}(OH)_3$, $Cr^{III}(OH)_3$, aqueous Cr(VI), Cr(III)-SRHA, aqueous Cr(III) and $FeCr_2O_4$ references. The near-edge spectra allow characterization of the valence state of Cr in the hotspots. Hexavalent Cr has a characteristic intense pre-edge peak at 5993 eV that corresponds to a bound state $1s\rightarrow3d$ electronic transition that results from the mixing of Cr(3d) and O(2p) orbitals; since this transition is symmetry-forbidden for octahedral $Cr(III)O_6$, the pre-edge of trivalent Cr does not contain this feature [44]. The 1s-3d pre-edge peak can be clearly seen in the spectrum of aqueous Cr(VI) and is absent in the Cr(III) reference compounds analyzed (Figure 5); the intensity of the pre-edge peak has been used to estimate relative abundances of Cr(III) and Cr(VI) in previous studies characterizing Cr speciation in mineral samples [44, 45]. No pre-edge feature is seen in the Cr K edge μ-XAS spectra collected for the Meadowlands soil samples (Fig. 5), indicating that Cr contained in the hotspots is in the 3+ valence state.

Inspection of the μ-XAS Cr spectra collected at the Cr hotspots in the Meadowlands samples indicate that they are all quite similar, except for some variation in the intensities of the XAS oscillations (Fig. 5). The strong similarities between the spectra suggest that these hotspots contain the same Cr species found in all soils. Comparison to the spectra of the reference compounds shows that the μ-XAS spectra closely match the spectrum of chromite ($FeCr_2O_4$; Fig. 5). The chromite Cr K edge spectrum is distinctly different from the Cr spectra of the other Cr reference compounds analyzed (Fig.5) as well as Cr(0) and $Cr_2O_3$ [35], and we therefore conclude that the Cr species found at the hotspot locations is $FeCr_2O_4$. The differences in the oscillation intensities between the μ-XAS spectra are likely due to self-absorption effects in the fluorescence data of these highly concentrated Cr spots

dampening the XAS signal.

Combined, the μ-SXRF and μ-XAS data presented in Figures 4 and 5 indicate the presence of small (μm sized) chromite ($FeCr_2O_4$) particles scattered throughout the mineral matrix of the marsh samples. Despite the obvious importance of chromite to the Cr speciation in these soils, the presence of additional Cr species can not be discounted, as the high intensity counts of the chromite hotspots in the XRF maps may mask the presence of more diffusely distributed Cr species in the soil matrix. The bulk XAS analyses discussed next will address this possibility.

### 3.4 Bulk XAS results

Bulk XAS characterizes the speciation of the element of interest as the average of species present weighted by abundance [46], and was used here to determine the overall speciation of Cr in the Meadowlands marsh soils. The normalized near-edge spectra of the bulk samples analyzed are presented in Figure 6a along with the spectra of the various Cr reference compounds. There is no evidence of the 1s-3d pre-edge feature characteristic of Cr(VI) in any of the soil samples, which indicates that soil Cr is predominantly in the 3+ valence state. The absence of Cr(VI) limits the solubility of Cr in these samples, and is consistent with the high organic matter content and generally wet conditions encountered in these marsh soils, which lead to low Eh conditions facilitating reduction of Cr(VI) to Cr(III).

Constraints on the average local chemical environment of Cr in the marsh soils are provided by comparison of the Cr K edge spectra of the soils and reference compounds. Figure 6b presents a zoom-in of the near edge region of the soil sample and reference spectra to facilitate comparison. The bulk Cr K edge spectra of samples 3A and 9 resemble the spectrum of chromite ($FeCr_2O_4$), although with reduced intensity of the oscillations due to self absorption effects, indicating chromite as the dominant Cr species in these samples, whereas the spectra of samples 1A and 1B are quite similar (although not

13

identical) to the spectrum of $Cr_{0.1}Fe_{0.9}(OH)_3$ (Fig. 6b), which indicates that a substantial portion of Cr

in these samples is incorporated in Fe(III)-hydroxide mineral phases; the spectra of samples 2A and 2B

share features with the spectra of both $Cr_{0.1}Fe_{0.9}(OH)_3$ and $FeCr_2O_4$, suggesting mixed Cr speciation.

The presence of substantial Fe(III)-hydroxide incorporated Cr(III) in these samples as evidenced by the

bulk XAS data is consistent with the positive correlation between Cr and Fe contents observed for these

soils (Fig. 1), and corroborates the results of the sequential extraction schemes showing appreciable

amounts of Cr associated with reducible soil components (Fig. 2). Thus, while the microbeam data

discussed above highlight the presence of chromite partilces in the soil materials, the bulk XAS data

indicate that the overall soil Cr speciation is influenced by Fe(III)-hydroxide-incorporated Cr(III) as

well, with variations between the soils as to the relative contributions of these species.

   As an experimental test of our interpretation of the bulk soil Cr spectra containing contributions

from $Cr_{0.1}Fe_{0.9}(OH)_3$ and chromite, we used hydroxylamine hydrochloride for the selective removal of

Fe-oxides from sample 1a according to step 3 of the Tessier extraction scheme (Table 1). The XAS

spectrum of the Fe-extracted sample is compared in Figure 7 to the spectrum of the original sample and

the spectra of $Cr_{0.1}Fe_{0.9}(OH)_3$ and chromite. Removal of Fe-oxides (and thus of Cr(III) incorporated in

$Fe(OH)_3$) has a notable effect on the Cr XAS spectrum of sample 1a, with the spectrum of the non-

extracted sample resembling the spectrum of $Cr_{0.1}Fe_{0.9}(OH)_3$, and the spectrum of the Fe-extracted

sample resembling chromite (Fig. 7). This result is consistent with the presence of a mixture of

$Cr_{0.1}Fe_{0.9}(OH)_3$ and chromite in the marsh soils.

   Further refinement of the Cr speciation in the soil samples involved linear combination (LC) fits

of the experimental bulk Cr XAS spectra of the soil samples. A principal component analysis (PCA) of

the spectral data set of the soil samples revealed three significant components, consistent with the

presence of three different Cr species in this data set. Target transformations indicated $Cr_{0.1}Fe_{0.9}(OH)_3$

and chromite as components, consistent with the results presented above. The spectrum of Cr(III)

associated with organic matter (Cr(III)-DOM in Fig. 5) was also identified as a potential component, although the target transformation for this component produced a lower fit quality than for the other Cr species, and the spectrum of aqueous Cr(III) was equally well suited as a component due to the strong similarity of the spectra of aqueous and organically complexed Cr(III) (Fig. 5). The small fraction of exchangeable and readily soluble Cr(III) determined in the sequential extractions, and the substantial contribution of organically complexed Cr(III) indicated by the Zeien-Brummer and Tessier schemes in particular (Fig. 2) are consistent with organically complexed Cr(III) rather than aqueous Cr(III) as the third Cr component in these soils. Linear combination fits of the experimental spectra using the Cr(III)-SRHA, $Cr_{0.1}Fe_{0.9}(OH)_3$ and chromite spectra as endmembers are shown in Figure 8. The LC analysis yielded reasonable fits of the experimental data, with estimated contributions of $Cr_{0.1}Fe_{0.9}(OH)_3$ ranging between 11% and 63%, chromite contributions ranging between 31 and 46 %, and organically complexed Cr contributions ranging between 8 and 56 % (Fig. 8). Spectral fits of samples 3A and 9 (not shown) indicated >80% of Cr present as chromite, but yielded poor fit quality as a result of self absorption dampening the chromite signal relative to the transmission spectrum of the chromite reference. Overall, the linear combination fits provide spectroscopic confirmation of the presence of multiple Cr species in these samples, as alluded to in the sequential extraction results. The fractions of Cr(III) associated with Fe-oxides and organic matter as determined from the linear combination fits showed no correlation with soil organic matter and Fe contents, and the differences between the soils as to the relative contributions  of the various Cr species present are thus not readily explained by soil properties. Differences in local weathering conditions, sedimentary deposit rates, and organic matter inputs may be among the factors determining the differences in Cr speciation between the sites.

## 4. DISCUSSION

The macroscopic and spectroscopic results of this study indicate a mixed Cr speciation in the

COPR marsh soils investigated, with contributions from chromite, Cr(III) incorporated into $Fe(OH)_3$, and organically complexed Cr(III). Chromite is an oxide mineral belonging to the spinel group. The mineral is found in mafic igneous rocks and metamorphic rocks, and is part of the original ore material from which COPR is derived [1]. Incomplete transformation of chromite into chromate during high temperature roasting results in the presence of residual chromite in COPR, as reported in several studies concerned with mineralogical characterization of COPR material [9, 16, 21]. Chrysochoou et al. [21] used μ-XAS and μ-SXRF to study the distribution and speciation of Cr in (unweathered) COPR material from New Jersey, and found small chromite particles scattered throughout the matrix of the original COPR material; similarly, Tinjum et al. [16] found chromite particles in the matrix of COPR from a site on the Midatlantic US coast from XRF analyses. No Cr(VI)-containing mineral phases are observed in the COPR soil characterized here. Studies on hydrated COPR material in the early stage of weathering have indicated calcium-aluminum chromate (CAC), hydrogarnets, and hydrotalcite phases as primary Cr(VI) host phases [4, 10, 11, 16, 20, 21]. The absence of Cr(VI)-rich minerals while chromite persists in these highly weathered COPR soils (with pH's < 7; Table 2) is consistent with results from experimental and thermodynamic studies showing that chromite is mostly inert towards dissolution under aqueous surface conditions in the pH range 4-12 , whereas main Cr(VI) host phases in COPR such as CAC and hydrogarnet dissolve at pH values < 7 [12, 16, 47]. Thus, the low overall Cr contents  and absence of remnant Cr(VI) in these weathered COPR soils is consistent with leaching of Cr(VI) from the site, facilitated by destabilization of Cr(VI) host phases and the high mobility of released $CrO_4^{2-}$ and $HCrO_4^-$ resulting from the weak particle reactivity of these oxyanions [48]. Additional factors affecting the Cr speciation and concentration in these topsoils are the low Eh and high organic matter contents of these marsh soils favoring reduction of Cr(VI) to Cr(III), and the deposition of sedimentary and organic material diluting the top soil Cr content.

In contrast to chromite, Cr(III) incorporated into $Fe(OH)_3$ and complexed with organic matter

are secondary reactions products of COPR weathering. Weathering of COPR under surface conditions releases Cr(VI) [12, 16], which may be reduced to Cr(III) under moderate to low Eh conditions; at the site studied here, reduction of Cr(VI) to Cr(III) is facilitated by generally wet conditions and high organic matter contents. The XAS data indicate that at least part of the Cr released is incorporated in Fe(III)-hydroxides and complexed by organic matter, resulting in an overall solid state Cr speciation that consists of $Cr_xFe_{1-x}(OH)_3$, organically complexed Cr(III), and residual chromite. Weathering of Fe-containing COPR minerals such as brownmillerite is likely a main source of Fe for $Fe(OH)_3$ precipitation, whereas organic matter inputs derive from vegetation growing at the site. Incorporation of Cr(III) in Fe(III)-hydroxides has been characterized in model studies, and involves substitution of Cr(III) at Fe(III) sites in the mineral structure [34, 49-51], which is facilitated by the similarity in size and charge of the trivalent Cr and Fe cations [52]. Incorporation of Cr(III) into secondary Fe(III)-(hydr)oxide minerals has been reported in studies dealing with Cr speciation in soils and Fe(0)-based permeable reactive barriers [40, 53-55]. Strong organic complexation of Cr(III) has been noted both in laboratory as well as field-based studies [40, 54, 56-58].

The presence of substantial $Cr_xFe_{1-x}(OH)_3$ implies strong potential for Cr (re)mobilization in these wetland soils. Following submergence of riparian soils, soil microbes switch to, among others, $Fe^{3+}$ atoms in Fe(III)-(hydr)oxides as terminal electron acceptors for respiration after depletion of $O_2$, leading to reductive dissolution of Fe(III)-hydroxide phases and release of associated contaminants [59]. At the time of sampling, the soils were oxic, but the water table was shallow, and the site is fully submerged for significant portions of the year (F. Artigas, personal communication). It is very likely that Cr release takes places during submergence as a result of the reductive dissolution of $Cr_xFe_{1-x}(OH)_3$. The fate of Cr(III) released during flooding requires further study, and the Cr speciation as characterized here should be considered a snapshot of the Cr speciation as it occurs during oxic periods of the wet-dry cycle of these wetland top soils. The formation of $Cr_xFe_{1-x}(OH)_3$ solids during soil

17

oxygenation as observed here suggests the presence of mobile Cr species under anoxic conditions that are available for incorporation in secondary $Fe(OH)_3$ precipitates as they form.

Of concern at the current site is the release of Cr(VI) from weathering COPR deposits deeper in the profile. The exact depth of the COPR deposits has not been established in the current study, but runs at least 1m deep as determined during sampling of the current sample set. The pH of samples taken from a depth of 30 cm was measured at 8.5-8.9, substantially higher than the pH values of the topsoil characterized here (although less than the pH 11.5-12 values of unweathered COPR), indicating that COPR weathering is less advanced deeper in the profile than in the surface layers. The inputs of organic acids and fresh rain and river water essentially dissolve and titrate the alkaline COPR deposits from the surface down. The potential of actively weathering COPR deposits deeper in the profile releasing Cr(VI) that may be transported to surface and groundwater requires further investigation.

We observe notable differences between the three sequential extraction schemes as to the relative and absolute amounts of Cr extracted in steps aimed at comparable Cr fractions. This finding underscores the fact that sequential extractions provide operationally defined speciation data that generally reflect trends and major differences in metal speciation between different soils, but do not necessarily provide accurate estimates of the concentrations of the various species targeted. Limitations of sequential extraction schemes include lack of extractant efficiency and selectivity, re-adsorption or precipitation of target species following mobilization, and changes in the valence of redox-sensitive target species during extraction [e.g. 29, 60, 61]. The differences in extraction results observed for the three schemes likely reflect differences in the selectivity and efficiency of extractants used to target the various Cr species. Of particular note in this respect is the presence of chromite particles in the materials studied. Clearly, none of the extraction schemes specifically targets this Cr species, and, perhaps more importantly, none of the schemes has been optimized to avoid extractant interaction with this Cr phase. The linear combination fits of the bulk XAS data (Fig. 8) indicate that a substantial

portion of soil Cr is present in chromite, so that any interaction between extractant chemicals and COPR residual is likely to affect the extraction results. The differences in Cr extraction results between the schemes may therefore be partly due to extractant interactions with Cr contained chromite which, ideally, would be part of the residual Cr fraction of all three schemes applied here. Additional speciation information obtained through complementary techniques is useful to interpret results from sequential extraction experiments, and can be used to tailor extraction schemes to optimize performance for a specific set of samples.

## 5. CONCLUSIONS

The speciation of Cr in marsh soils from the New Jersey Meadowlands developed in weathering chromite ore processing residue (COPR) was characterized using a combination of sequential extractions and synchrotron-based microbeam and bulk X-ray absorption spectroscopic (XAS) analyses. Results from the sequential extraction experiments point to low solubility of soil Cr based on small amounts of Cr extractable with water and mildly acidic solutions. The extractions further indicated substantial Cr associated with reducible and oxidizable soil components, as well as non-extractable residual Cr. Notable differences between the three extraction schemes as to the absolute and relative amounts of Cr extracted in comparable steps indicate differences in the selectivity and efficiency of extractants used, and underscore the operationally defined nature of Cr speciation provided by these methods. Micro X-ray fluorescence maps in combination with $\mu$-XAS data collected on the soil materials indicated the presence of $\mu$m-sized chromite ($FeCr_2O_4$) particles scattered throughout the weathered COPR soil matrix. These particles are remnants from the original ore from which the COPR derived representing ore material that was not transformed to chromate during high temperature ore roasting. The chromite particles have relatively high resistance towards weathering and persist in the weathered COPR material, while Cr(VI), which is associated with less stable COPR

19

minerals such as hydrogarnets and hydrotalcites, is no longer present in the weathered surface layers. Bulk XAS data collected on the soils showed the presence of Cr(III) incorporated in $Fe(OH)_3$ precipitates, and Cr(III) associated with soil organic matter, indicating (partial) repartitioning of mobilized Cr into secondary phases. The results from this study show that these topsoils represent highly weathered COPR material, developed in response to inputs of organic acids and rain and river water that dissolve and titrate the alkaline COPR deposits from the surface down. The low Cr contents of the weathered material (200-800 ppm) compared to unweathered COPR (up to 60,000 ppm) indicate that substantial Cr leaching takes place during COPR weathering, with part of the released Cr incorporated in secondary $Fe(OH)_3$ or complexed with organics. The presence of $Cr_xFe_{1-x}(OH)_3$ in the marsh soils studied implies strong potential for Cr remobilization as a result of reductive dissolution during periods of flooding; the effect of anoxia on Cr speciation, and the potential of active COPR weathering releasing Cr(VI) deeper in the profile requires further study.

**REFERENCES**

[1] T. Burke, J. Fagliano, M. Goldoft, R.E. Hazen, R. Iglewicz, T. McKee, Chromite ore processing

residue in Hudson County, New Jersey,  Environm. Health Perspect. 92 (1991) 131–137.

[2] G. Darrie,  Commercial extraction technology and process waste disposal in the manufacture of chromium chemicals from ore, Env. Geochem. Health 23 (2001) 187-193.

[3] J.G. Farmer, R.P. Thomas, M.C. Graham, J.S. Geelhoed, D.G. Lumsdon, E. Paterson, Chromium speciation and fractionation in ground and surface waters in the vicinity of chromite ore processing residue disposal sites, J. Env. Monitoring 4 (2002) 235-243.

[4] M. Chrysochoou,  D. Dermatas, M. Asce, D.G. Grubb, M. Asce, D.H. Moon, C. Christodoulatos, Importance of mineralogy in the geoenvironmental characterization and treatment of chromite ore processing residue, J. Geotechn. Geoenv. Engin. 36 (2010) 510-521.

[5] New Jersey Department of Environmental Protection (NJDEP) 1997.  Hudson County chromate chemical production sites: Background: http://www.nj.gov/dep/srp/siteinfo/chrome/bkgrnd.htm

[6] B.R. James, The challenge of remediating chromium contaminated soil, Env. Sci. Technol. 30 (1996) 248A – 251A.

[7] J.G. Farmer, M.C. Graham, R.P. Thomas, C. Licona-Manzur, E. Paterson, C.D. Campbell, J.S. Geelhoed, D.G. Lumsdon, J.C.L. Meeussen, M.J. Roe, A. Connor, A.E. Fallick, R.F.J. Bewley, Assessment and modelling of the environmental chemistry and potential for remediative treatment of chromium contaminated land, Environ. Geochem. Health 21 (1999), 331–337.

[8] T.E. Higgins, A.R. Halloran, M.E. Dobbins, A.J. Pittignano, In situ reduction of hexavalent

chromium in alkaline soils enriched with chromite ore processing residue, J.Air Waste Management

Assoc. 48 (1998), 1100-1106.


[9] R.P. Thomas, S.J. Hillier, M.J. Roe, J.S. Geelhoed, M.C. Graham,  E. Paterson, J.G. Farmer,

Analytical characterisation of solid- and solution-phase chromium species at COPR- contaminated

sites, Environ. Geochem. Health. 6 (2001)  2–9.


[10] S. Hillier, M.J. Roe,  J.S. Geelhoed, A.R. Fraser, J.G. Farmer, E. Paterson, Role of quantitative

mineralogical analysis in the investigation of sites contaminated by chromite ore processing residues,

Sci. Total Environ. 308 (2003) 195–210.


[11] M. Chrysochoou, S.B. Fakra, M.A. Marcus, D.H. Moon DH, D. Dermatas, Microstructural

analyses of Cr(VI) speciation in chromite ore processing residue (COPR),  Env. Sci. Technol. 43

(2009) 5461-5466.


[12] J.S. Geelhoed, J.C.L. Meeussen, S. Hillier, D.G. Lumsdon,  R.P. Thomas,  J.G. Farmer, E.

Paterson,  Identification and geochemical modeling of processes controlling leaching of Cr(VI) and

other major elements from chromite ore processing residue, Geochim. Cosmochim. Acta 66 (2002),

3927-3942.


[13] J.S. Geelhoed, J.C.L. Meeussen, D.G. Lumsdon, S. Hillier, M.J. Roe, R.P. Thomas, R.J.F. Bewley,

J.G. Farmer, E. Paterson, Modelling of chromium behaviour and transport at sites contaminated with

chromite ore procesing residue: Implications for remediation methods, Env. Geochem.Health 23 (2001)

261-265.

[14] C.H. Weng, C.P. Huang, H.E. Allen, A.H.D. Cheng, P.F. Sanders, Chromium leaching behavior in soil derived from chromite ore processing waste, Sci.Total Env. 33 (1994) 71-86.

[15] C.H. Weng, C.P. Huang, P.F. Sanders, Effect of pH on Cr(VI) leaching from soil enriched in chromite ore processing residue, Env. Geochem. Health 23 (2001) 207-211.

[16] J.M. Tinjum, C.H. Benson, T.B. Edit, Mobilization of Cr(VI) from chromite ore processing residue through acid treatment, Sci.Total Env. 391 (2008), 13-25.

[17] C.M. Su, R.D. Ludwig RD, Treatment of hexavalent chromium in chromite ore processing solid waste using a mixed reductant solution of ferrous sulfate and sodium dithionite, Env. Sci. Technol. 39 (2005) 6208-6216.

[18] A.M. Graham, A.R. Wadhawan, E.J. Bouwer, Chromium occurrence and speciation in Baltimore harbor sediments and porewater, Baltimore, Maryland, USA, Env. Toxicol. Chem. 28 (2009) 471-480.

[19] M. Chrysochoou, D. Dermatas,  Application of the Rietveld method to assess chromium(VI) speciation in chromite ore processing residue,  J. Haz. Mat. 141 (2007) 370-377.

[20] S. Hillier, D.G. Lumsdon, R. Brydson, E. Paterson, Hydrogarnet: a host phase for Cr(VI) in Chromite Ore Processing Residue (COPR) and other high pH wastes, Environ. Sci. Technol. 41 (2007) 1921–1927.

[21] M. Chrysochoou, D.H.  Moon, S. Fakra, M. Marcus M, D. Dermatas, C. Christodoulatos, Use of micro X-ray absorption spectroscopy  and diffraction to delineate Cr(VI) speciation in COPR, Global NEST J. 11 (2009) 318-324.

[22] M. Wazne, S.C. Jagupilla, D.H. Moon, C. Christodoulatos, A. Koutsopyros, Leaching mechanisms of Cr(VI) from chromite ore processing residue, J. Env. Quality 37 (2008) 2125-2134.

[23]  J.S. Geelhoed, J.C.L. Meeussen, M.J. RoE, S. Hillier, R.P. Thomas, J.G. Farmer, E. Paterson, Chromium remediation or release? Effect of iron(II) sulfate addition on chromium(VI) leaching from columns of chromite ore processing residue, Env. Sci. Technol. 37 (2003) 3206-3213.

[24] G.W. Thomas, Soil pH and Soil Acidity, in: D.L. Sparks (ed.) Methods of Soil Analysis Part 3: Chemical Methods, Soil Science Society of America Book Series, Madison Wisconsin, 1996, pp 712-755.

[25] D.W. Nelson, L.E. Sommers, Total carbon, organic carbon, and organic matter, in: D.L. Sparks (Ed.) Methods of Soil Analysis Part 3: Chemical Methods,  Soil Science Society of America Book Series, Madison Wisconsin, 1996, pp. 961-1010.

[26] A.M. Ure, Ph. Quevauviller, M. Muntau, B. Griepink, Speciation of heavy metals in soils and sediments: An account of the improvement and harmonization of extraction techniques undertaken under the auspices of the BCR of the Commission of the European Communities, International J. Env. Analytical Chem. 51 (1993) 135-151.

[27] A. Tessier, P.G.C. Campbell, M. Bisson, Sequential extraction procedure for the speciation of particulate trace metals, Analytical Chem. 51 (1979) 844

[28] H. Zeien, G.W. Brummer, Chemische Extraktion zur Bestimmung von Schwermetallbindungsformen in Boden, Mitteilungen der Deutschen Bodenkundlichen Gesellschaft 59 (1989) 505-510.

[29] A.C. Scheinost, R. Kretzschmar, S. Pfister, D.R. Roberts, Combining selective sequential extractions, x-ray absorption spectroscopy, and principal component analysis for quantitative zinc speciation in soil, Env. Sci.Technol. 36 (2002) 5021-5028.

[30] A. Voegelin, G. Tokpa, O. Jacquat, K. Barmettler, R. Kretzschmar, Zinc fractionation in contaminated soils by sequential and single extractions: Influence of soil properties and zinc content, J. Env. Quality 37 (2008) 1190-1200.

[31] S. Tokalioglu, S. Karal S, L. Elci, Determination of heavy metals and their speciation in lake sediments by flame atomic absorption spectrometry after a four-stage sequential extraction procedure, Analytica Chim. Acta 413 (2000) 33-40.

[32] A.V. Filgueiras, I. Lavilaa, C. Bendicho, Chemical sequential extraction for metal partitioning in environmental solid samples, J. Env. Monitoring 4 (2002) 823-857.

[33] J.M. Ablett, C.C. Kao, R.J. Reeder, Y. Tang, A. Lanzirotti, X27A - A new hard X-ray micro-

spectroscopy facility at the National Synchrotron Light Source, Nuclear Instruments & Methods in Physics Related Research Section A: Accelerators, Spectrometers, Detectors and Associated Equipment 562 (2006): 487-494.

[34] Y. Tang, F.M. Michel, L. Zhang, R. Harrington, J. Parise, R.J. Reeder, Structural properties of the Cr(III)-Fe(III)-(oxy)hydroxide solid solution, Chem. Materials (2010), accepted pending revision.

[35] M.L. Werner, P.S. Nico, M.A. Marcus, C. Anastasio, Use of micro-XANES to speciate chromium in airborne fine particles in the Sacramento Valley, Env. Sci. Technol. 41 (2007) 4919-4924.

[36] T. Ressler, WinXAS: A new software package not only for the analysis of energy- dispersive XAS data,  J. Physique IV 7 (1997), C2-269.

[37] S.R. Wasserman, P.G. Allen, D.K. Shuh, J.J. Bucher, N.M.  Edelstein, EXAFS and principal component analysis: a new shell game, J. Synchrotron Radiation 6 (1999) 284-286.

[38] M. Nachtegaal,M.A. Marcus, J.E.  Sonke, J. Vangronsveld, K.J.T. Livi, D. Van der Lelie, D.L.Sparks, Effects of in situ remediation on the speciation and bioavailability of zinc in a smelter contaminated soil, Geochim. Cosmochim. Acta 69 (2005) 4649-4664.

[39] D.H. McNear,,R.L. Chaney, D.L.Sparks, The effects of soil type and chemical treatment on nickel speciation in refinery enriched soils: A multi-technique investigation, Geochim. Cosmochim. Acta 71 (2007) 2190-2208.

[40] E. Doelsch, G. Moussard, H. Saint Macary, Fractionation of tropical soilborne heavy metals – Comparison of two sequential extraction procedures, Geoderma 143 (2008) 168-179.

[41] A. Sahuquilo, A. Rigol, G. Rauret, Overview of the use of leaching/extraction tests for risk assessment of trace metals in contaminated soils and sediments, TrAc trends Analytical Chem. 22 (2003) 152-159.

[42] M.J. McLaughlin, B.A. Zarcinas, D.P. Stevens, N. Cook, Soil testing for heavy metals, Commun.Soil Sci. Plant Analysis 31 (2000) 1661-1700.

[43] P. Quevaullir, G. Rauret,  B. Griepink, Conclusions of the workshop single and sequential extraction in sediments and soils, International J. Env.Analytical Chem. 51 (1993) 231-235.

[44] M.L. Peterson, G.E. Brown, G.A. Parks, C.L.Stein, Differential redox and sorption of Cr(III,VI) on natural silicate and oxide minerals: EXAFS and XANES results, Geochim. Cosmochim. Acta 61 (1997) 3399-3412.

[45] M.L. Peterson, G.E. Brown, G.A. Parks, Direct XAFS evidence for heterogeneous redox reaction at the aqueous chromium/magnetite interface, Colloids Surfaces A 107 (1996), 77-88.

[46] S.E. Fendorf, D.L. Sparks, G.M. Lamble, M.J. Kelley, Applications of X-ray absorption fine-structure spectroscopy to soils, Soil Sci. Soc.Am. J. 58 (1994) 1583-1595.

[47] C. Oze, S. Fendorf, D.K. Bird, R.G. Coleman, Chromium geochemistry in serpentized ultramafic

rocks and serpentine soils from the Franciscan Complex of California, Am. J. Sci. 304 (2004) 67-101.

[48] S.E. Fendorf, Surface reactions of chromium in soils and waters, Geoderma 67 (1995) 55-71.

[49] L. Charlet, A. Manceau, X-ray absorption spectroscopic study of the sorption of Cr(III) at the oxide-water interface. 2. Adsorption, coprecipitation and surface precipitation on hydrous ferric oxide, J. Colloid Interface Sci. 148 (1992) 443-458.

[50] A. Manceau, M.L. Schlegel, M. Musso, V.A. Sole, C. Gauthier, P.E. Petit, F. Trolard, Crystal chemistry of trace elements in natural and synthetic goethite, Geochim. Cosmochim. Acta 64 (2000) 3643-3661.

[51] C.M. Hansel, B.W. Wielinga, S. Fendorf, Structural and compositional evolution of Cr/Fe solids after indirect chromate reduction by dissimilatory iron-reducing bacteria, Geochim. Cosmochim. Acta 67 (2003) 401-412.

[52] B.M. Sass, D. Rai, Solubility of amorphous chromium(III)-iron(III) hydroxide solid solutions, Inorg. Chem. 26 (1987) 2228-2232.

[53] D. Fandeur, F. Juillot, G. Morin, L. Olivi, A. Cognigni, J.P. Ambrosi, F. Guyot, E. Fritsch, Synchrotron-based speciation of chromium in an oxisol from New Caledonia: Importance of secondary Fe-oxyhydroxides, Am. Mineralogist 94 (2009) 710-719.

[54] E. Doelsch, I. Basile-Doelsch, J. Rose, A. Masion, D. Borschneck, J.L. Hazemann, H. Saint

Macaray, J.Y. Borrero, New combination of EXAFS spectroscopy and density fractionation for the speciation of chromium within an andosol, Env. Sci. Technol. 40 (2006) 7602-7608.

[55] B. Flury, J. Frommer, U. Eggenberger, U. Mader, M. Nachtegaal, R. Kretzschmar, Assessment of long-term performance and chromate reduction mechanisms in a field scale permeable reactive barrier, En. Sci. Technol. 43 (2009) 6786-6792.

[56] B.R. James, R.J. Bartlett, Behavior of chromium in soils. V. Fate of organically complexed Cr(III) added to soil, J. Environ. Quality 12 (1983) 169-172.

[57] B.R. James, R.J. Bartlett, Behavior of chromium in soils. VI. Interactions between oxidation-reduction and organic complexation, J. Environ. Quality 12 (1983) 173-176.

[58] Y.L. Wei, Y.C. Lee, H.F. Hsieh, XANES study of Cr sorbed by a kitchen waste compost from water, Chemosphere 61 (2005) 1051-1060.

[59] D.L. Sparks, Environmental Soil Chemistry. Academic Press, San Diego, California, 2002.

[60] M.J. La Force, S. Fendorf, Solid-phase iron characterization during common selective sequential extractions, Soil Sci. Soc. Am. J. 64 (2000) 1608-1615.

[61] J.D. Ostergren, G.E. Brown, G.A. Parks, T.N.Tingle, Quantitative speciation of lead in selected mine tailings from Leadville, CO, Environ. Sci.Technol. 33 (1999) 1627-1636

Table 1. Sequential extraction procedures used in this study to speciate Cr in the marsh soils.

| Scheme | Step[a] | Operationally defined Cr fraction | Extractant solution and volume [b] | Operating conditions |
|---|---|---|---|---|
| BCR | 1 | Acid soluble | 0.11 M HOAc (40 mL) | 16 h at 25 C |
| | 2 | Associated with reducible soil compounds | 0.1 M NH2OH-HCl, pH 2 (40 mL) | 16 h at 25 C |
| | 3 | Associated with oxidizable soil compounds | 30% w/v H2O2 (10 mL – evaporation) | 1h at 85 C |
| | | | 30% w/v H2O2 (10 mL – evaporation) | 1h at 85 C |
| | | | 1 M NH4OAc (50 mL) | 16 h at 25 C |
| Tessier | 1 | Exchangeable | 1M MgCl2, pH 7 (8 mL) | 1 h at 25 C |
| | 2 | Acid soluble | 1M NaOAc, pH 5 (25 mL) | 5 h at 25 C |
| | 3 | Associated with reducible soil compounds | 0.04M NH2OH-HCl & 25% w/w HOAc (20 mL) | 6 h at 96 C |
| | 4 | Associated with oxidizable soil compounds | 0.02 M HNO3 (3 mL) + 30% w/v H2O2 (5 mL) | 2 h at 85 C |
| | | | 30% w/v H2O2 (3 mL) | 3h at 85 C |
| | | | 3.2M NH4OAc (5 mL) | 30 min at 25 C |
| Zeien-Brummer | 1 | Carbonate bound, soluble, and readily mobilizable complexes | 1.0 M NH4-acetate, pH 6 (25 mL) | 24 h at 25 C |
| | 2 | Mn(IV)-oxide bound | 1M NH2OH-HCl (12.5mL) + 1.0M NH4-acetate (12.5 mL) | 30 min at 25 C |
| | 3 | Organically bound | 0.025 M NH4-EDTA, pH 4.6 (25 mL) | 90 min at 25 C |
| | 4 | Associated with weakly crystalline Fe(III) oxides | 0.2 M NH4-oxalate, pH 3.25 (25 mL) | 2 h at 25 C (dark) |
| | 5 | Associated with crystalline Fe(III)-oxides | 0.1M ascorbic acid (12.5 mL) + 0.2 M NH4-oxalate (12.5 mL), pH 3.25 | 2 h at 96 C |

[a] Residual (non-extractable) Cr was determined using micro-wave assisted $HNO_3$ digestion following the extraction sequence; [b] Extractant volume is based on 1 g of soil material

Table 2. Chemical characteristics of the marsh soil samples.

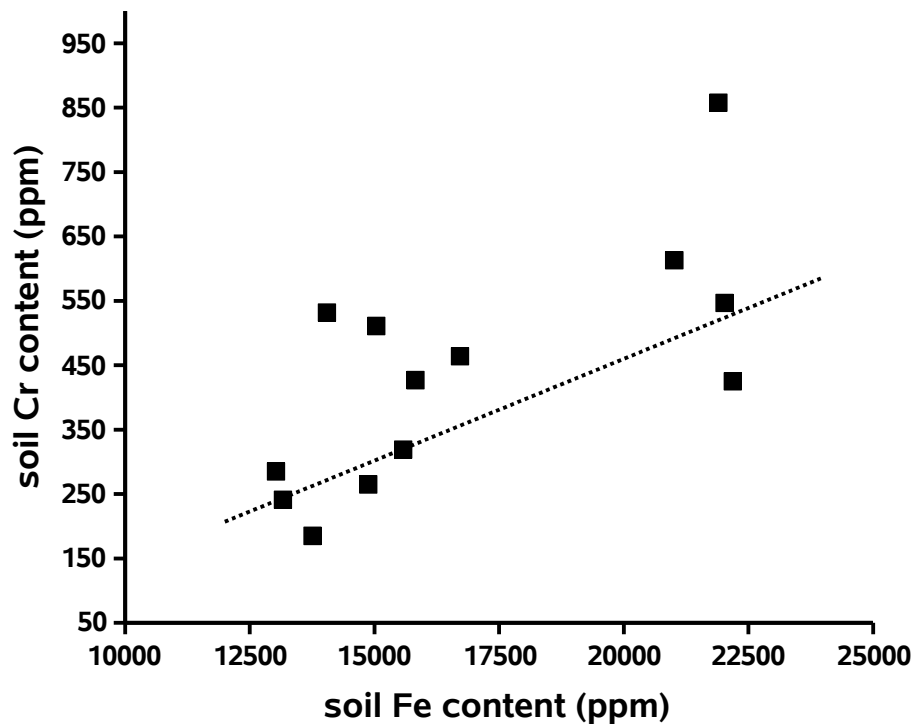| Sample | pH | [Cr] (mg/kg) | [Fe] (mg/kg) | Org. Matter (%) |
|--------|------|-----|-------|------|
| 1a | 4.67 | 858 | 21897 | 11.2 |
| 1b | 5.07 | 613 | 21013 | 11.3 |
| 2a | 5.58 | 464 | 16716 | 18.1 |
| 2b | 6.71 | 427 | 15822 | 19.1 |
| 3a | 6.43 | 532 | 14047 | 24.7 |
| 3b | 6.41 | 511 | 15037 | 24.8 |
| 5a | 4.5 | 547 | 22022 | 20.9 |
| 6a | 5.96 | 185 | 13758 | 14.6 |
| 6b | 5.53 | 285 | 13028 | 22.1 |
| 9 | 5.64 | 425 | 22184 | 22.2 |
| 10a | - | 265 | 14878 | 24.6 |
| 10b | 5.74 | 319 | 15579 | 19.1 |
| 10c | 5.7 | 241 | 13166 | 19.3 |

**Figure captions.**

Figure 1. Correlation between the Fe and Cr contents of the marsh soil samples (n=13) collected for this study. The least squares fit (dashed line; $R^2$=0.49) is given by $y = 0.0316x - 172.24$.

Figure 2. Results from the sequential extraction experiments: (A) BCR scheme; (B) Tessier scheme and (C) Zeien-Brummer scheme. The Cr fractions have been normalized to the sum of the residual and total extracted Cr concentrations for each soil, which were within 15% of the total Cr soil contents reported in Table 1 determined separately by micro-wave assisted $HNO_3$ extraction.
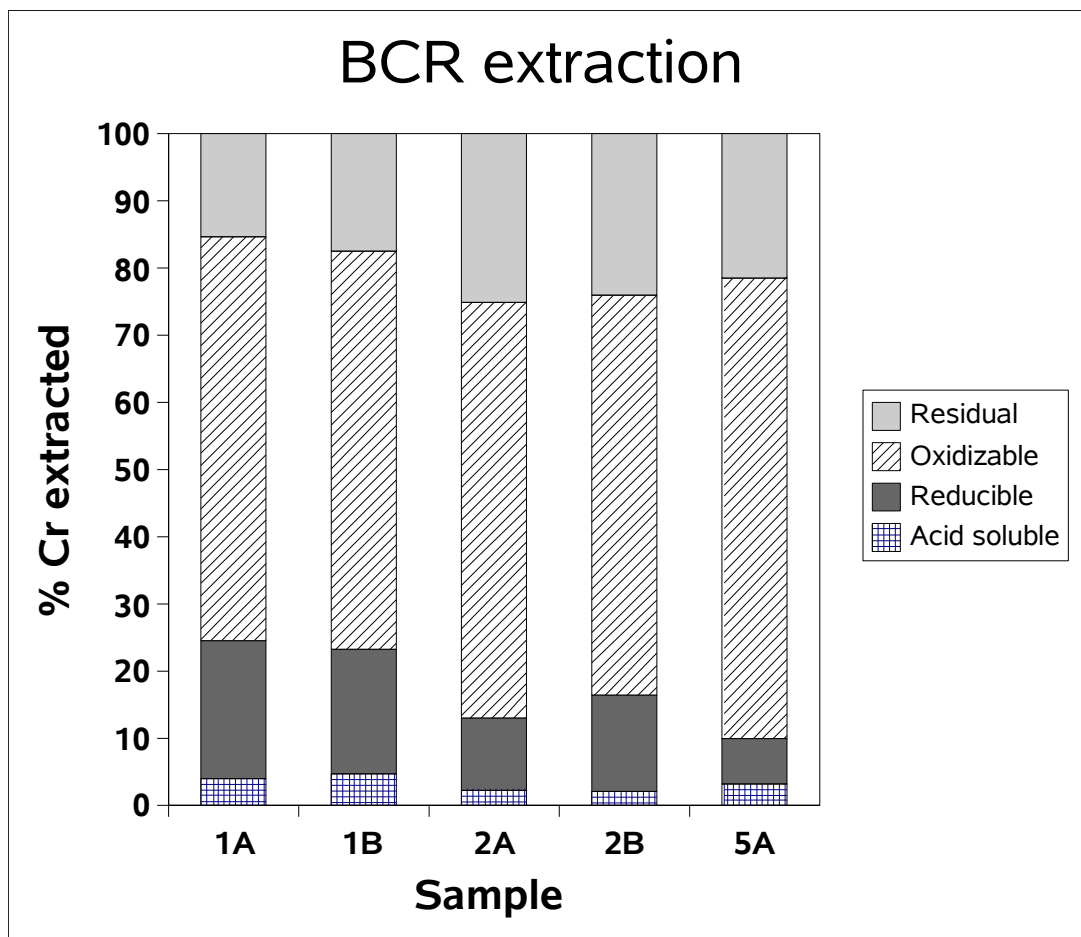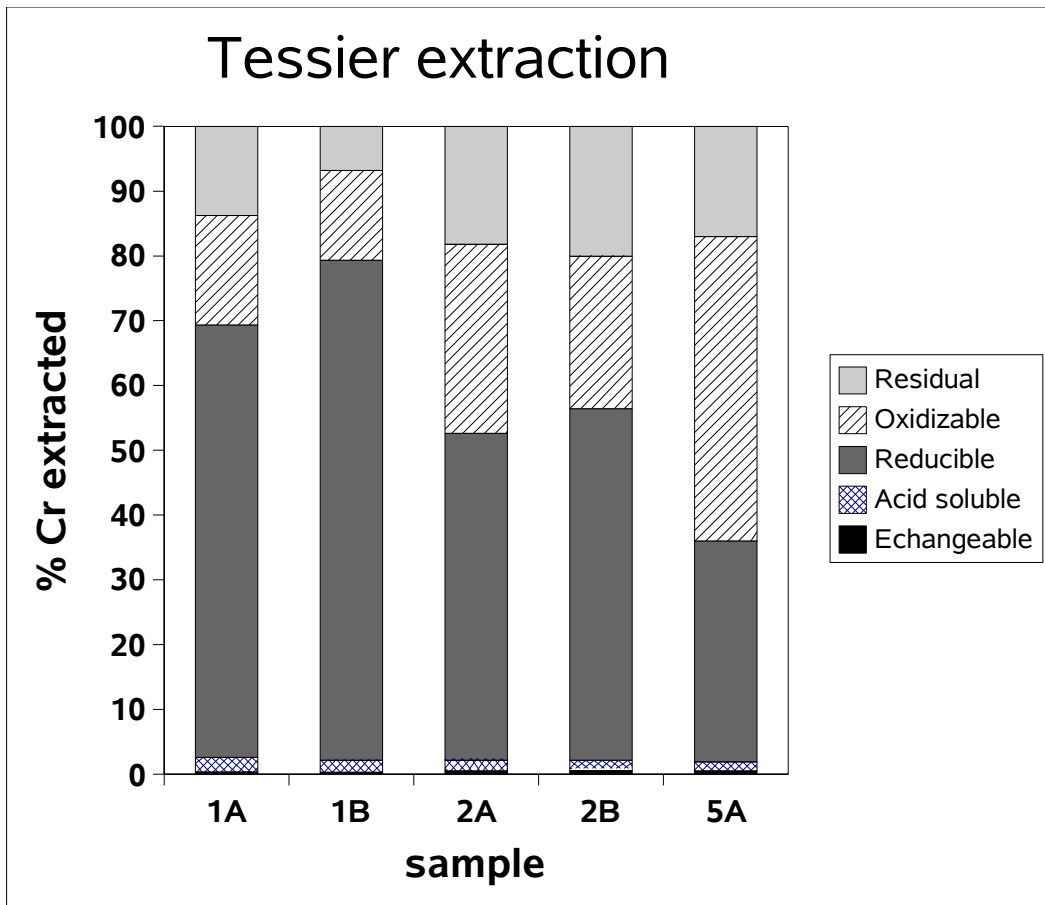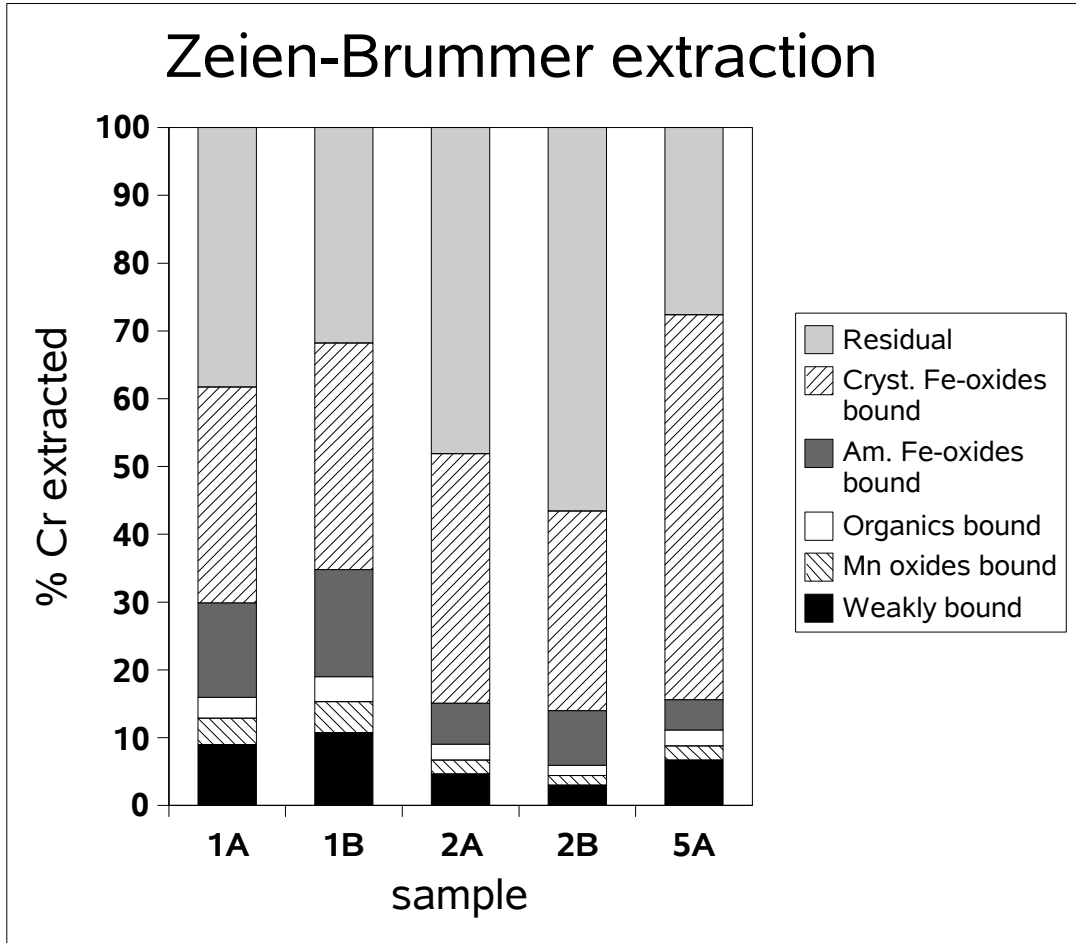
Figure 3. Correlation plots of Cr fractions extracted in comparable steps in the three extraction schemes: (A) exchangeable and acid soluble Cr; (B) Cr associated with oxidizable soil components or organic matter; (C) Cr associated with reducible soil components or Fe(III)- and Mn(IV)-oxides, and (D) residual Cr. On the y-axes, "ZB" indicates Zeien-Brummer extraction results.
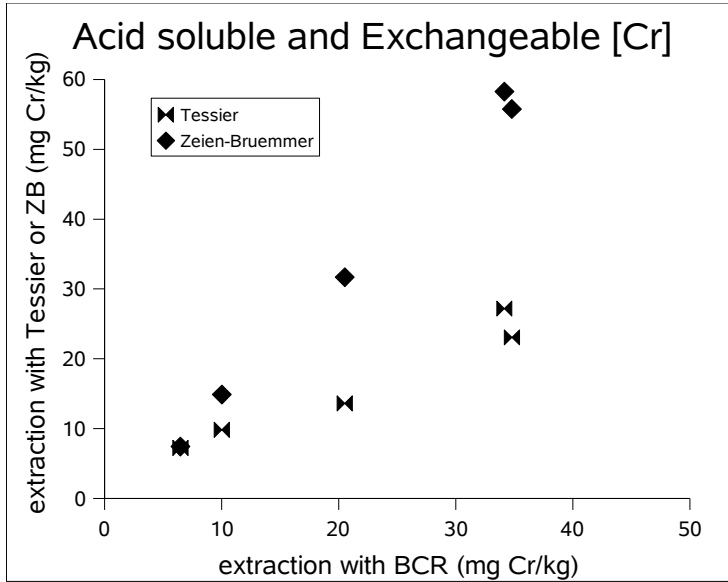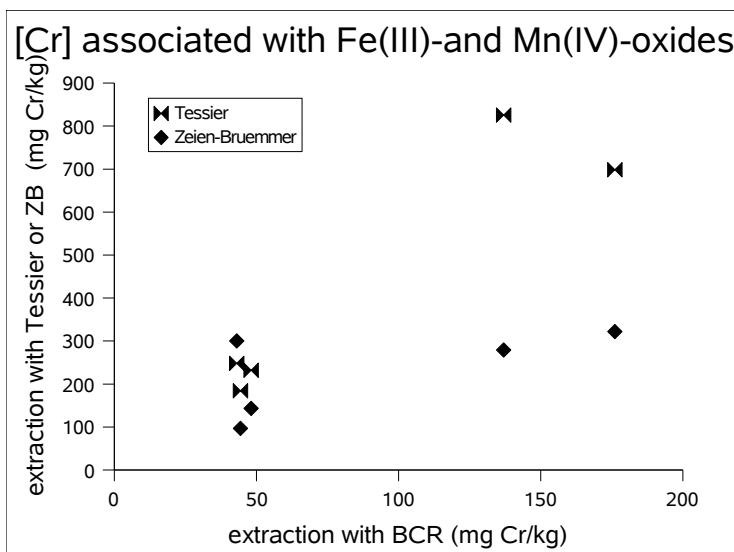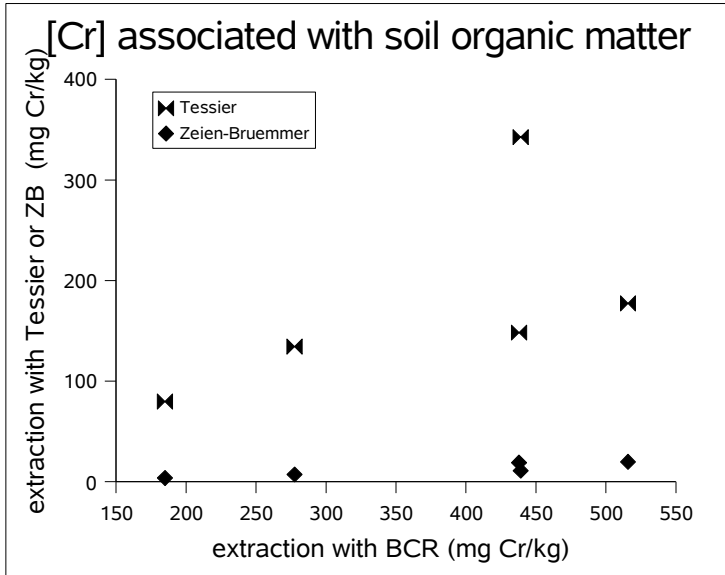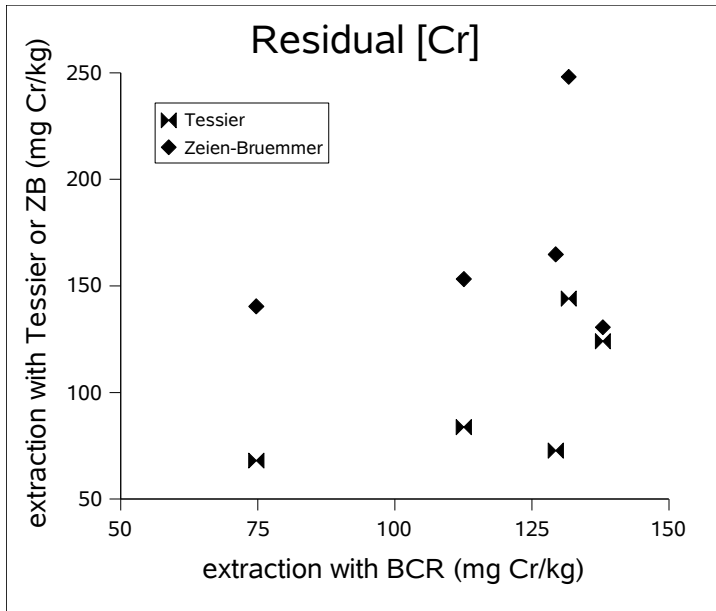
Figure 4. Synchrotron X-ray fluorescence maps of the distribution of Ca, Fe and Cr in samples 1A, 3A and 5A. Bright colors represent high concentrations, dark colors represent low concentrations. Numbers indicate Cr hotspot locations where microfocused Cr K edge spectra were collected.

Figure 5. Comparison of the Cr near edge spectra collected at the various Cr hotspots to the spectra of Cr reference compounds, including aqueous Cr(III) – organic complexes (Cr(III)-DOM), Cr(III) incorporated into $Fe(OH)_3$ ($Cr_{0.1}Fe_{0.9}(OH)_3$ and $Cr_{0.3}Fe_{0.7}(OH)_3$ ), and chromite ($Cr_2FeO_4$). A description of the Cr reference spectra is provided in the text.

Figure 6. Bulk Cr K edge XAS spectra of the marsh samples and Cr reference compounds: (A) full spectra; (B) zoom-in of the near-edge region.

Figure 7. Comparison of the Cr K edge spectrum of sample 1A before and after extraction of Fe(III)-oxides; the spectra of $Cr_{0.1}Fe_{0.9}(OH)_3$ and chromite are included for reference.

Figure 8. Linear combination (LC) fits (dashed lines) of the bulk XAS spectra (solid lines) of samples 1A, 1B, 2A, 2B and 5A using chromite, $Cr_{0.1}Fe_{0.9}(OH)_3$ and Cr(III)-DOM as endmembers. The proportions of the endmember spectra to the linear combination fit are indicated for each sample.

Figure 1. Correlation between the Fe and Cr contents of the marsh soil samples (n=13) collected for this study. The least squares fit (dashed line; $R^2$=0.49) is given by y=0.0316x-172.24.

Figure 2.  Results from the sequential extraction experiments: (A) BCR scheme; (B) Tessier scheme and  (C) Zeien-Brummer scheme. The Cr fractions have been normalized to the sum of the residual and total extracted Cr concentrations for each soil, which were within 15% of the total Cr soil contents reported in Table 1 determined separately by micro-wave assisted $HNO_3$ extraction.
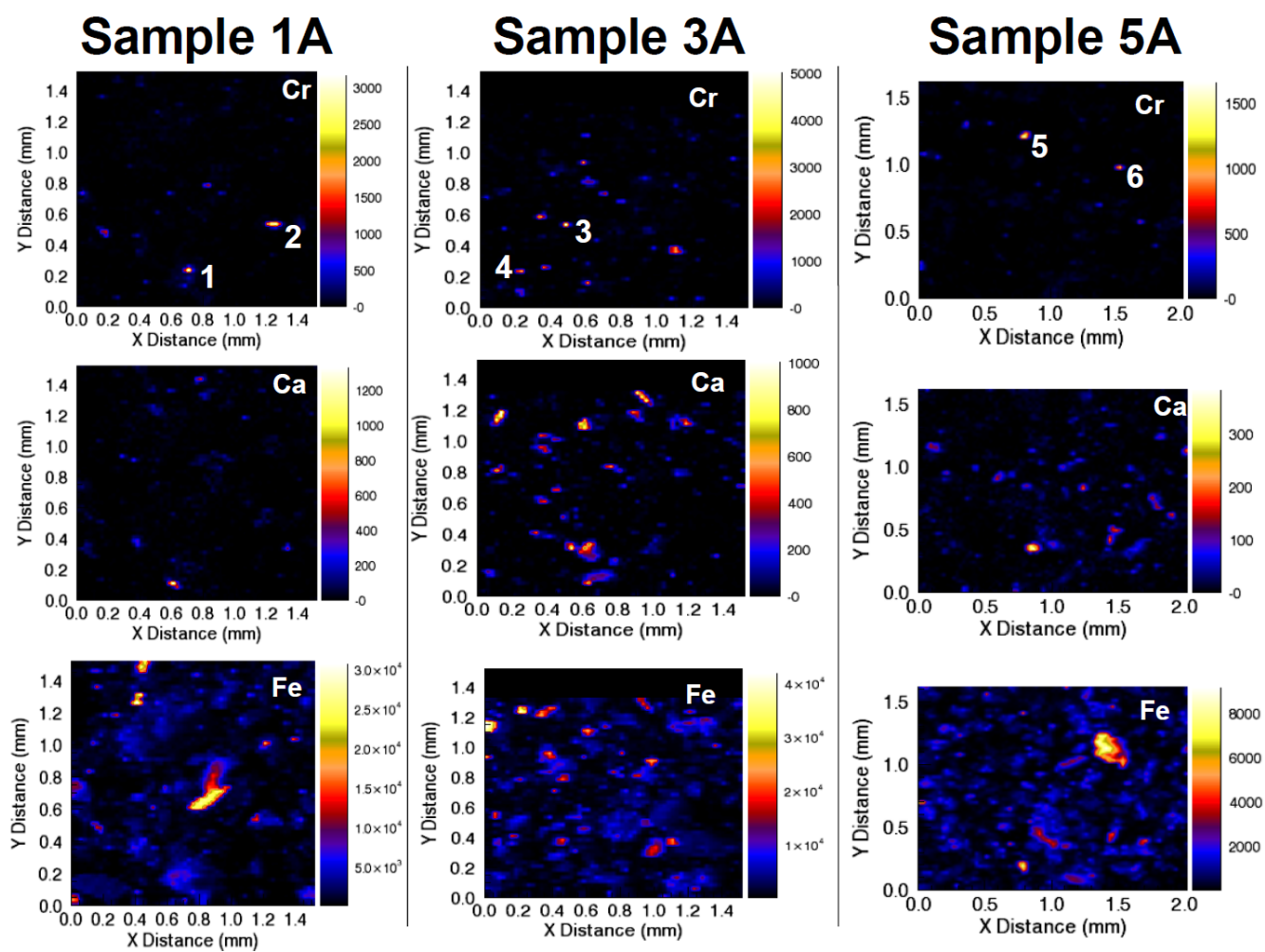


Figure 2A

Figure 2B

Figure 2C

Figure 3. Correlation plots of Cr fractions extracted in comparable steps in the three extraction schemes: (A) exchangeable and acid soluble Cr; (B) Cr associated with oxidizable soil components or organic matter; (C) Cr associated with reducible soil components or Fe(III)- and Mn(IV)-oxides, and (D) residual Cr. On the y-axes, "ZB" indicates Zeien-Brummer extraction results.



Figure 3A



Figure 3B

Figure 3C



Figure 3D

Figure 4. Synchrotron X-ray fluorescence maps of the distribution of Ca, Fe and Cr in samples 1A, 3A and 5A. Bright colors represent high concentrations, dark colors represent low concentrations. Numbers indicate Cr hotspot locations where microfocused Cr K edge spectra were collected.

Figure 5. Comparison of the Cr near edge spectra collected at the various Cr hotspots to the spectra of Cr reference compounds, including aqueous Cr(III) – organic complexes (Cr(III)-DOM), Cr(III) incorporated into $Fe(OH)_3$ ($Cr_{0.1}Fe_{0.9}(OH)_3$ and $Cr_{0.3}Fe_{0.7}(OH)_3$ ), and chromite ($Cr_2FeO_4$). A description of the Cr reference spectra is provided in the text.

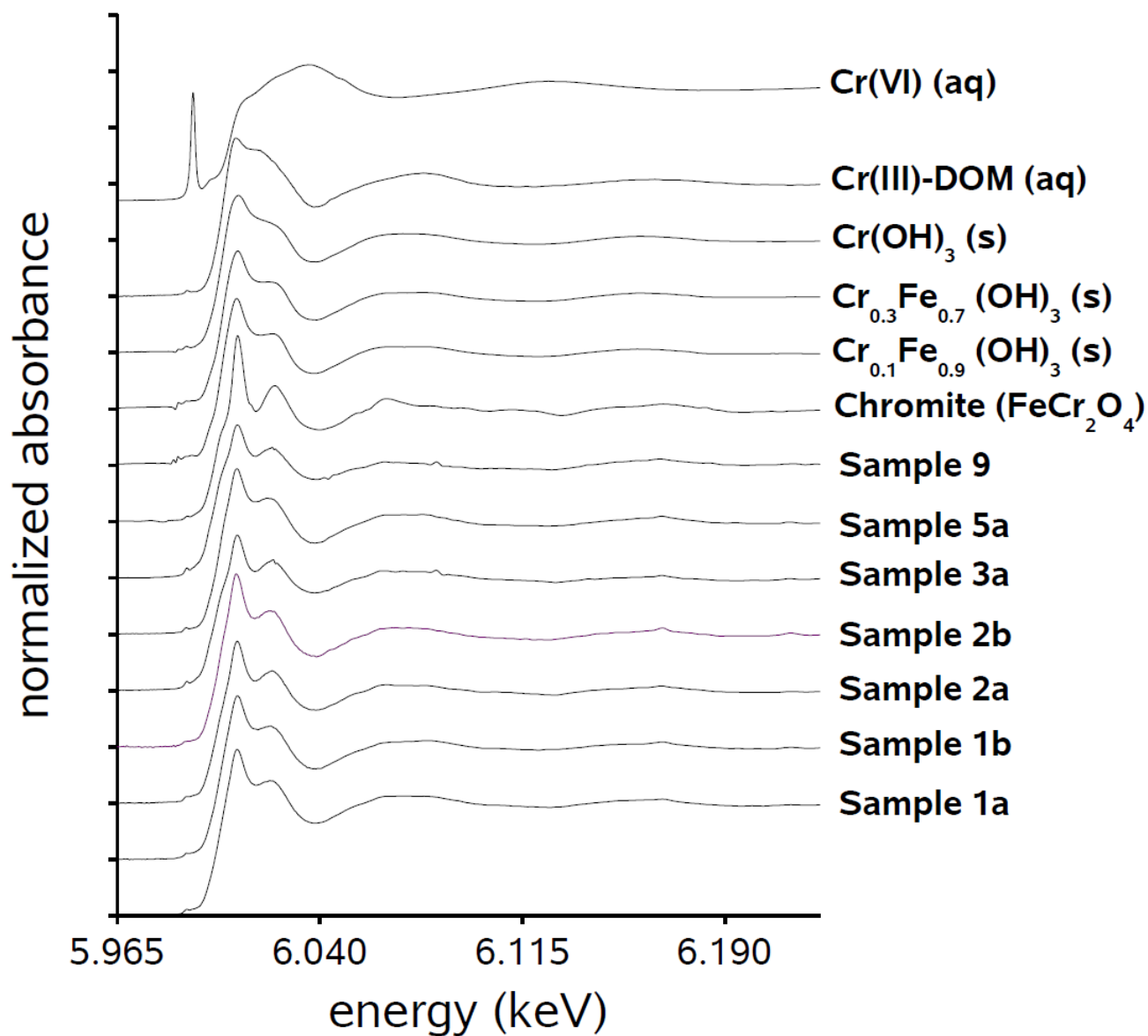Figure 6. Bulk Cr K edge XAS spectra of the marsh samples and Cr reference compounds: (A) full spectra; (B) zoom-in of the near-edge region.
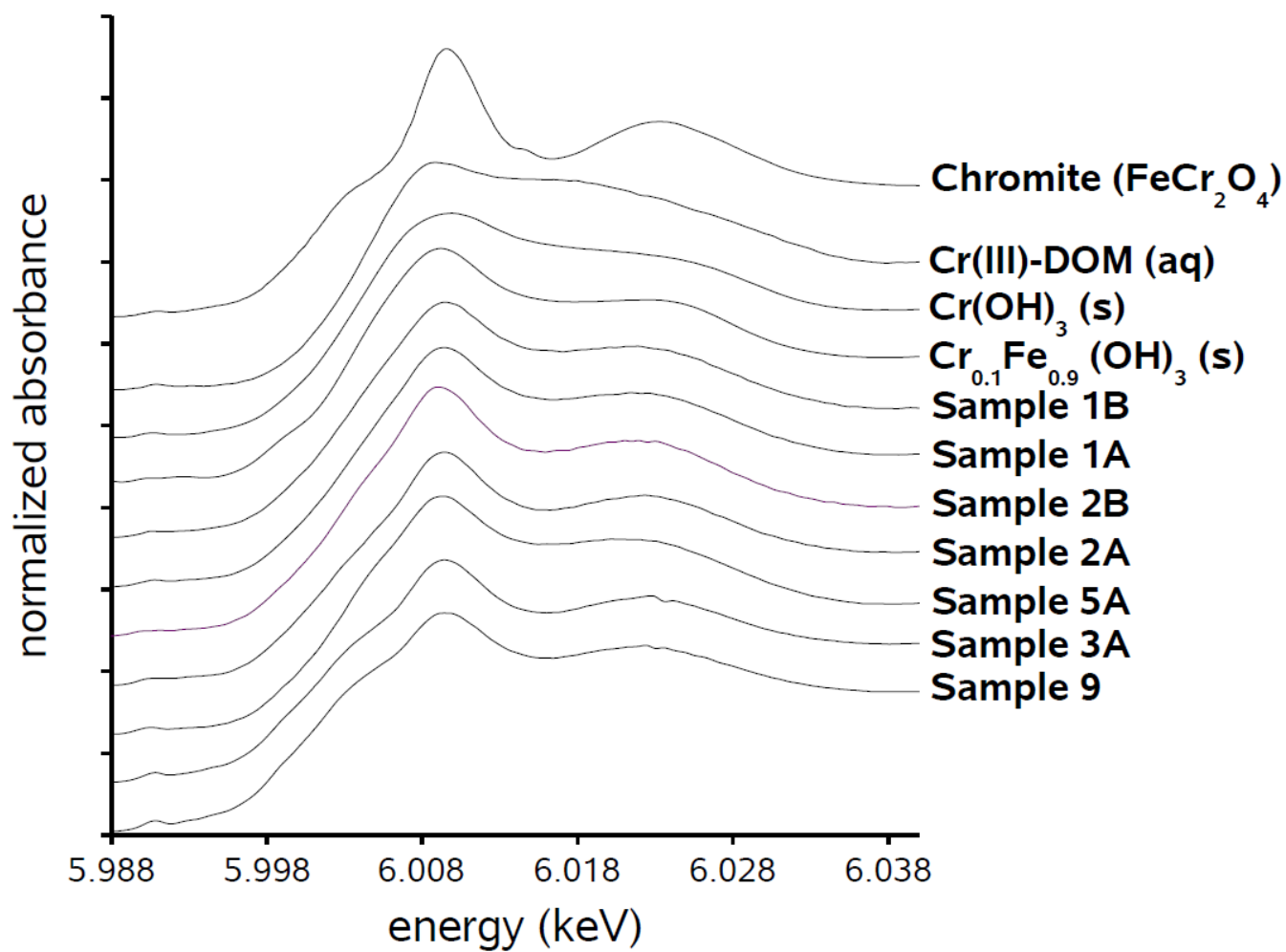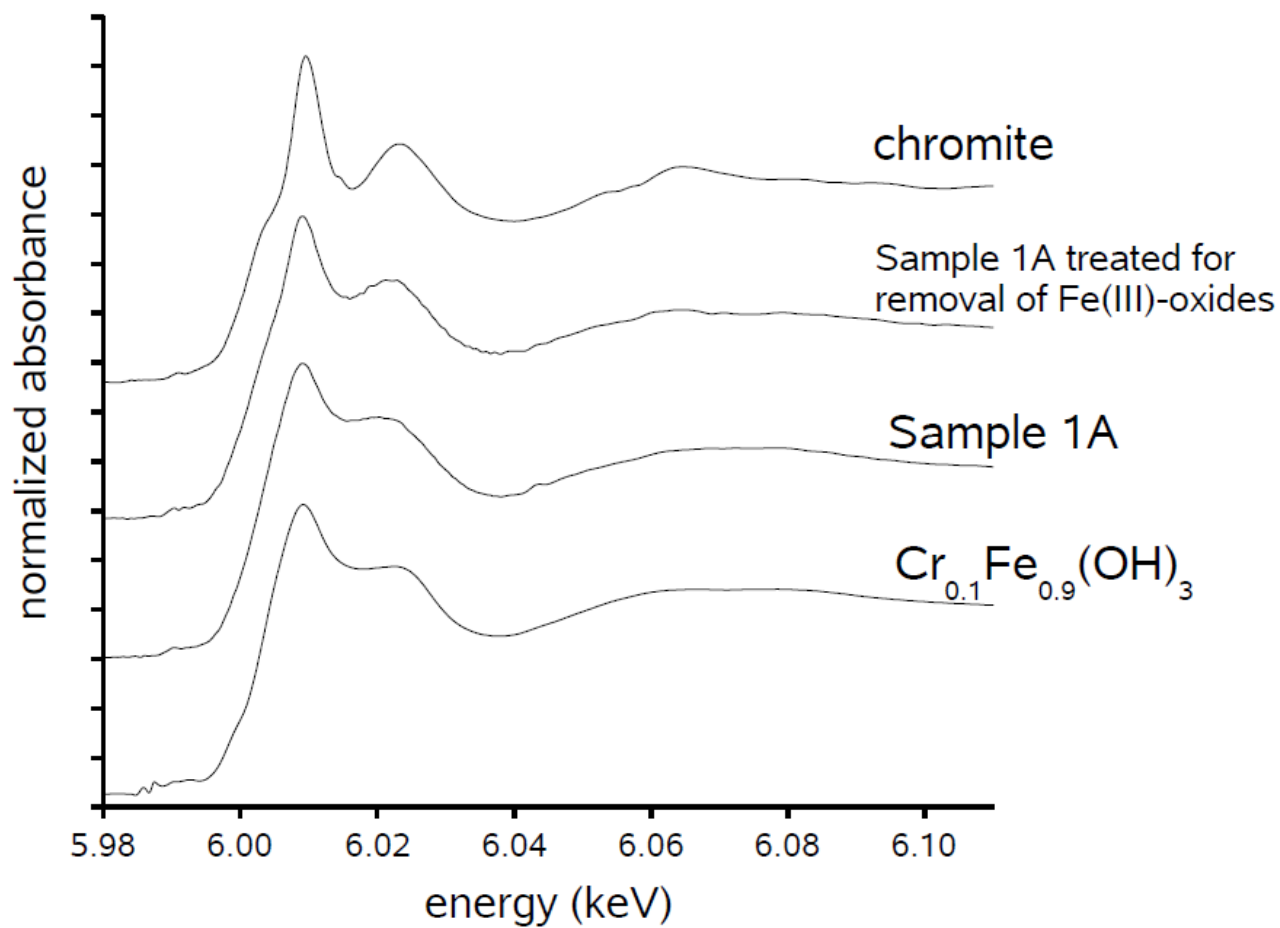


Figure 6A

Figure 6B

Figure 7. Comparison of the Cr K edge spectrum of sample 1A before and after extraction of Fe(III)-oxides; the spectra of $Cr_{0.1}Fe_{0.9}(OH)_3$ and chromite are included for reference.
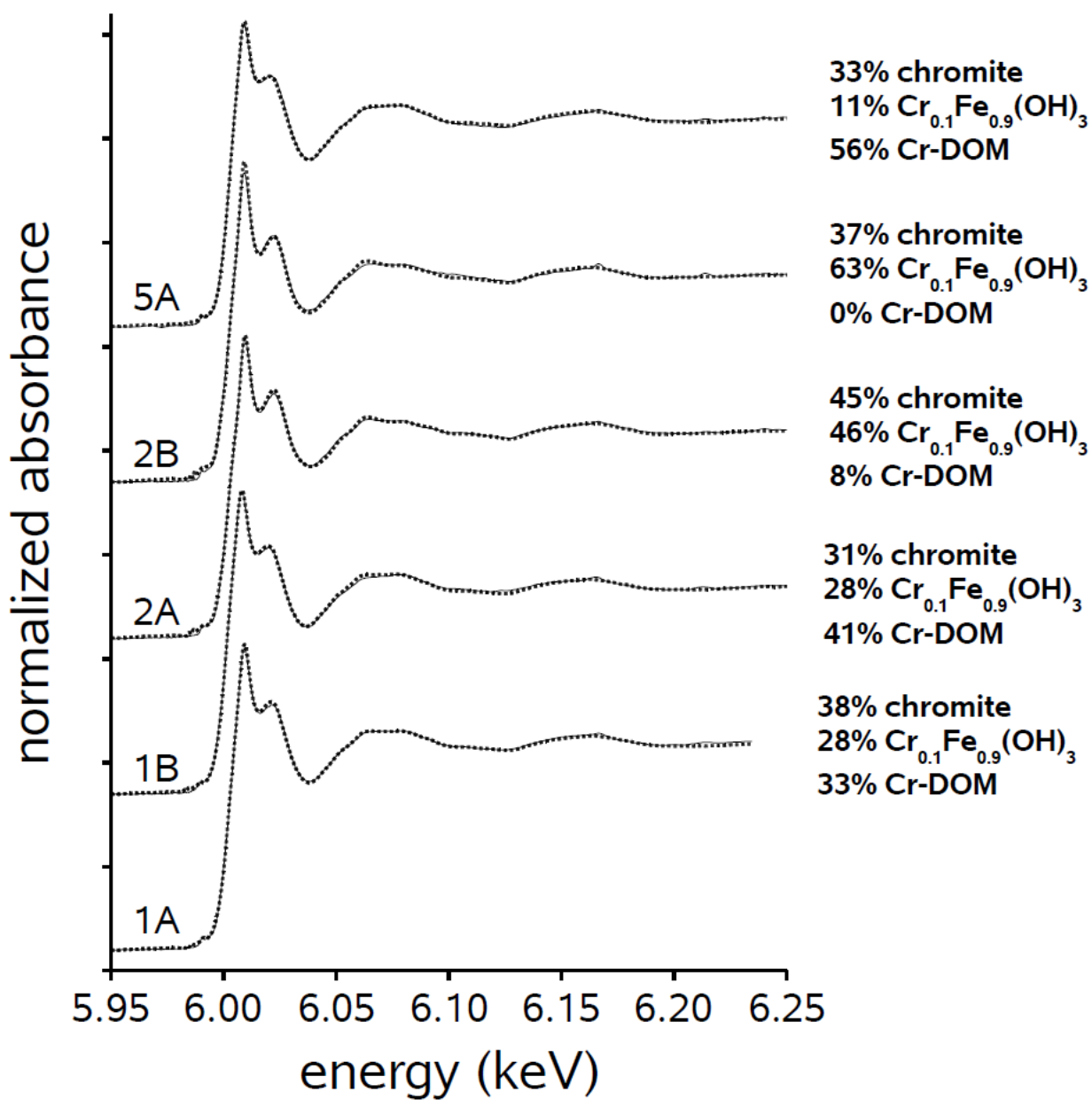
Figure 8. Linear combination (LC) fits (dashed lines) of the bulk XAS spectra (solid lines) of samples 1A, 1B, 2A, 2B and 5A using chromite, $Cr_{0.1}Fe_{0.9}(OH)_3$ and Cr(III)-DOM as endmembers. The proportions of the endmember spectra to the linear combination fit are indicated for each sample.